

On the response of simple reactors to regular trains of pulses

Jakub Siewewiesiuk^a and Jerzy Górecki^{ab}

^a Institute of Physical Chemistry, Polish Academy of Sciences, Kasprzaka 44/52, 01-224 Warsaw, Poland. E-mail: kudas@ichf.edu.pl

^b ICM UW, Pawińskiego 5A, 02-106 Warsaw, Poland. E-mail: gorecki@ichf.edu.pl

Received 18th October 2001, Accepted 21st January 2002

First published as an Advance Article on the web 12th March 2002

Propagating pulses of concentration in an excitable system may carry information because regions of high concentration of a selected reagent may be associated with one logical state, and regions of low concentration with another. Spatially distributed reactors constructed of active (excitable) and passive areas in which reagents diffuse can be applied to transform such information. In this paper we consider a few examples of such reactors (a chemical diode, a cross junction switch) and study their response to a chemical input of high frequency. We demonstrate that the response of a signal processing device may depend on the input frequency.

1 Introduction

It has been recently recognized that nonlinear chemical systems may be used to process information. A review on the implementation of logic functions and computation by means of homogeneous chemical kinetics was presented by Hjelmfelt and Ross.¹ The authors investigated biochemical mechanisms to determine which parts of the reaction scheme may carry out such functions. In this approach the logical network is built of cyclic enzymatic reactions,² which are coupled *via* common reagents. Alternatively, in spatially distributed systems the travelling pulses of reagent concentration, which can be produced in excitable or oscillatory media, carry information, because the area of high concentration of a particular reactant may be considered as corresponding to the logical “true” state, whereas the area of low concentration corresponds to the logical “false”. This idea was used to construct simple chemical reactors with multiple inputs which perform the basic logical functions (AND, OR, NOT).^{3,4}

Reactors composed of “active” regions, in which reactions occur, and “passive” areas, where some of the reagents are absent and so only a part of the reactions proceed there, can perform more complex signal processing operations. Such reactors can be built using membranes; and the active areas are filled with an immobilized catalyst, whereas the passive areas do not contain it. A specially selected asymmetric geometry of the junction of two active areas allows one to develop⁵ and construct⁶ a chemical diode, which transmits pulses only in one direction. A circular excitable field with radial input and output channels can be used as a memory cell.⁷ In our recent work^{8,9} we have shown that a cross junction of active and passive areas may work as a switch of direction of propagation for a pulse of excitation.

However, in the studies mentioned above the response of a signal processing device with respect to a single input has been investigated. Such a situation describes a low frequency of the input signal, for which the reactor is fully relaxed when the next pulse arrives. In our recent paper¹⁰ we have shown that a passive barrier separating two excitable areas can transform the frequency of trains of pulses and that the transforming properties of a passive gap depend on the incoming signal fre-

quency. As a passive gap is an element of more complex devices, it seems worth while to study their response to high frequency trains of pulses.

This paper is organized as follows. In Section 2 we discuss the frequency transforming properties of a passive barrier, introduce the models used in this study [FitzHugh–Nagumo (FH-N) type model⁵ and Rovinsky–Zhabotinsky (R-Z) model^{9,11,12} of the Belousov–Zhabotinsky reaction] and describe the numerical technique. Section 3 deals with the behavior of chemical diodes and cross junctions in both FH-N and R-Z models exposed to regular trains of pulses. In the final section we summarize the results.

2 The frequency transforming properties of a passive barrier for selected models of chemical excitable systems

In our numerical calculations we are concerned with two models, a FitzHugh–Nagumo (FH-N) type model and the Rovinsky–Zhabotinsky (R-Z) model of the Belousov–Zhabotinsky reaction.

2.1 The FitzHugh–Nagumo (FH-N) type model

In the version of the FitzHugh–Nagumo model that we use, the dynamics in the active areas is described by the following equations:^{5,13,14}

$$\tau \frac{\partial u}{\partial t} = -\gamma[ku(u - \alpha)(u - 1) + v] + D_u \nabla^2 u \quad (1)$$

$$\frac{\partial v}{\partial t} = \gamma u \quad (2)$$

with the parameters $\tau = 0.03$, $\gamma = 1$, $k = 3.0$, $\alpha = 0.02$ (as given by Motoike and Yoshikawa⁵) and $D_u = 0.00045$.⁸ For these values of parameters the system has one stationary solution $(u, v) = (0, 0)$, which is excitable. The variables u and v cannot be directly associated with the concentrations of chemical species, but their behavior resembles that of an activator (u) and inhibitor (v).

We assume that in the passive areas no reaction occurs and only diffusion of the activator is possible; thus it is natural to call these regions “diffusion areas”. The equations describing the time evolution of u and v in these areas are as follows:⁵

$$\tau \frac{\partial u}{\partial t} = D_u \nabla^2 u \quad (3)$$

$$v = 0 = \text{const.} \quad (4)$$

with $\tau = 0.03$ and $D_u = 0.000\,45$, as in the excitable areas. Pulses are produced by locally decreasing the value of v to $v_{\text{ini}} = -0.8$.

2.2 The Rovinsky–Zhabotinsky (R-Z) model of the BZ reaction

This model was proposed by A. B. Rovinsky and A. M. Zhabotinsky as a description of the Belousov–Zhabotinsky reaction.^{11,12} It is based on the well known Field–Körös–Noyes^{15,16} mechanism¹² completed by the hydrolysis of bromomalonic acid to tartronic acid.¹¹ The Rovinsky–Zhabotinsky model uses two variables, x and z , corresponding to dimensionless concentrations of the activator HBrO_2 and of the oxidized form of the catalyst $\text{Fe}(\text{phen})_3^{3+}$. In the active regions, which contain the catalyst, the time evolution of the concentrations of x and z is described by eqns. (5) and (6):

$$\frac{\partial x}{\partial \tau} = \frac{1}{\varepsilon} \left[x(1-x) - \left(2q\alpha \frac{z}{1-z} + \beta \right) \frac{x-\mu}{x+\mu} \right] + \nabla_\rho^2 x \quad (5)$$

$$\frac{\partial z}{\partial \tau} = x - \alpha \frac{z}{1-z} \quad (6)$$

In the passive regions, without catalyst, the concentrations of x and z evolve according to eqns. (7) and (8):

$$\frac{\partial x}{\partial \tau} = -\frac{1}{\varepsilon} \left(x^2 + \beta \frac{x-\mu}{x+\mu} \right) + \nabla_\rho^2 x \quad (7)$$

$$z = 0 = \text{const.} \quad (8)$$

Eqns. (5)–(8) correspond to a typical experimental situation in which the catalyst is immobilized on a membrane, whereas the activator is in the solution and it can diffuse (compare refs. 6,17). Therefore, we assume free boundary conditions between the active and passive areas.

All variables and coefficients in eqns. (5)–(8) are dimensionless and the real concentrations of HBrO_2 and $\text{Fe}(\text{phen})_3^{3+}$ (X, Z) are related to (x, z) in the following way:

$$X = \frac{k_1 A}{2k_4} x \quad (9)$$

$$Z = Cz \quad (10)$$

where $k_{\pm i}$ denote the rate constants of the corresponding reactions in the Field–Körös–Noyes model,^{11,12,15,16} $A = [\text{HBrO}_3]$ and $C = [\text{Fe}(\text{phen})_3^{2+}] + [\text{Fe}(\text{phen})_3^{3+}]$. The coefficients (α , β , μ , ε) are defined in refs. 9 and 11, and they can be expressed by $k_{\pm i}$, the concentrations of reagents and the value of the Hammett acidity function (h_0),^{18,19,20} describing the effective proton concentration expressed in mol l^{-1} .

In our numerical calculations for the BZ system we use the same values of parameters as considered in refs. 11, 12 and 21: $A = 0.02\text{ M}$, $C = 0.001\text{ M}$, $k_1 = 100\text{ M}^{-2}\text{ s}^{-1}$, $k_4 = 1.7 \times 10^4\text{ M}^{-2}\text{ s}^{-1}$ and $q = 0.5$. The corresponding values of scaled parameters α , β , ε and μ are $0.017h_0^{-2}$, $0.0017h_0^{-1}$, 0.1176 and $0.000\,51$, respectively. For these values of parameters the system described by eqns. (5) and (6) becomes excitable if $h_0 < 0.9899$.²¹ As in ref. 9 we have chosen $h_0 = 0.5$.

The relationships between the dimensionless units of time τ and distance ρ used in eqns. (5)–(8) and the real time t and distance r are the following:

$$t = \frac{k_4 C}{k_1^2 A^2 h_0} \tau \quad (11)$$

$$r = \sqrt{\frac{k_4 C}{h_0} \frac{1}{k_1 A}} \sqrt{D_X} \rho \quad (12)$$

where D_X is the diffusion constant of the activator x . For the parameters chosen:

$$t/\text{s} = 8.5\tau \quad (13)$$

$$r/\text{cm} = 2.915 \sqrt{D_X/\text{cm}^2\text{ s}^{-1}} \Delta\rho \quad (14)$$

The diffusion constant depends strongly on the medium in which the reactions proceed. In aqueous solution it is of the order of $10^{-5}\text{ cm}^2\text{ s}^{-1}$,^{6,11,18,20,21} whereas for a reaction in a gel it may be reduced by two orders of magnitude.^{6,22} In order to make our results more general we present all distances and velocities in the double form: dimensionless, and as a function of the ratio of diffusion constants D_X/D_{X_0} , where the value of D_{X_0} corresponds to the particular choice of the diffusion constant $D_{X_0} = 1 \times 10^{-5}\text{ cm}^2\text{ s}^{-1}$.^{11,12} The second number allows one to see more clearly the real spatial and temporal scales of the considered process.

For the values of parameters defined above, the stationary concentrations of x and z in the active area are

$$x_{\text{sa}} = 7.283 \times 10^{-4} \quad (15)$$

$$z_{\text{sa}} = 1.060 \times 10^{-2} \quad (16)$$

[which is the stationary solution of eqns. (5) and (6)] and the stationary concentrations in the passive area [which is the stationary solution of eqns. (7) and (8)] are

$$x_{\text{sp}} = 5.010 \times 10^{-4} \quad (17)$$

$$z_{\text{sp}} \equiv 0 \quad (18)$$

We initiate the pulses by locally increasing the value of x to $x_{\text{ini}} = 0.1$.

2.3 The frequency transforming on a single passive barrier

At the beginning let us summarize the results we have recently obtained.¹⁰ Let us consider a plane of the active chemical medium divided into two subplanes by a strip of a passive medium. Let us assume that a single pulse propagating in the excitable area arrives at the strip from the perpendicular direction. It is easy to guess what may happen. If the barrier is narrow, it is transparent to the pulse, which means that the pulse arriving at one side of it excites the active area on the other side. If the barrier is wide, the pulse does not get through. The maximum width of a transparent barrier is called the “penetration depth” (p_d). However, the problem of penetration through the barrier becomes more interesting if we consider a train of arriving pulses with high enough frequency f_1 that consecutive pulses within the train can no longer be treated as well separated in time.

In order to study the response of a passive barrier to a chemical signal of high frequency, we consider excitable pulses on a one-dimensional interval (Fig. 1). The interval of length l is divided into n equal parts by $n+1$ points of a lattice, including both ends. In Fig. 1 the grey lines correspond to active (excitable) media, and the passive medium (the barrier), indicated with a black line, is located between nodes n_1 and n_2 ($1 \ll n_1 < n_2 \ll n$). It means that the evolution of the system at all nodes $j \in [0, n_1] \cup [n_2, n]$ is given by one set of reaction–diffusion equations (corresponding to the active/excitable medium), and another set (corresponding to the passive med-

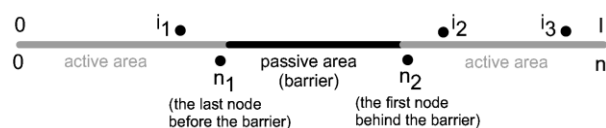


Fig. 1 The scheme of the system used to investigate the properties of a passive barrier. The grey bars correspond to active areas, and the black bar stands for the barrier. The barrier is located between nodes n_1 and n_2 (excluding n_1 and n_2). The value of u (for the FH-N model) or x (for the R-Z model) is observed at nodes i_1 , i_2 and i_3 .

ium) gives the evolution at all nodes $i \in (n_1, n_2)$. Thus, the barrier's width is estimated as

$$d \cong (n_2 - n_1 - 1)dl \quad (19)$$

where

$$dl = l/n \quad (20)$$

There are free flow boundary conditions between passive and active media, and no flux boundary conditions at both ends of the interval. Initially both active and passive areas are in their stationary states. Pulses of excitation are initiated at the left end of the interval and they travel to the right, coming across the passive barrier on their way. The method of initiating the pulses depends on the investigated model (it may be done by decreasing the inhibitor concentration or by increasing the activator concentration). We focus our attention on trains of pulses which are initiated regularly at times kt_p , where $k = 1, 2, 3, \dots, k_{\max}$ and $t_p > 0$ is a constant. In the following we distinguish the "incoming signal" or "input signal" (a train of pulses coming into the considered device, e.g. a barrier) and the "outgoing signal" or "output signal" (a train of pulses coming out of the device). We can define the input signal frequency as $f_1 = 1/t_p$.

The concentrations of reagents of interest are calculated using the implicit method based on the Crank–Nicolson discretization of the Laplace operator.²³ The distance between neighboring nodes ($dl = l/n$) is the space step of the numerical integration. In our computations we have used several values of dl and time step (dt) to verify the numerical stability of our results.

The concentrations of selected reagents are recorded at indicators located at the nodes i_1 (before the barrier), i_2 (just behind the barrier) and i_3 (far behind the barrier), as shown on Fig. 1. By comparing the time evolution of concentrations at i_1 , i_2 and i_3 we can tell whether a pulse which arrives at the barrier is able to cross it. Moreover, by counting the number of maxima of concentration within a certain time interval, we can measure the frequency of the incoming and the outgoing chemical signals (f_1 and f_2 respectively). To describe quantitatively the change in chemical signal frequency for given f_1 and d , we introduce the "filtering ratio" defined as f_2/f_1 .

The range of d , in which the frequency transforming may be observed, is finite as there always exists a barrier of width d_1 narrow enough to be transparent to all pulses in a train and another one impenetrable for any of them (with a width of d_0). Thus the nontrivial transforming properties of the passive barrier may be observed only in some finite range of d , which depends on the selected model and the values of its parameters. In calculations for the FH-N model [eqns. (1)–(4)] we have found^{8,10} that the penetration depth is about $d_0 \approx 0.163$. In the case of the R-Z model [eqns. (5)–(8)] we have found¹⁰ that the penetration depth for a single pulse d_0 is about $3.295 [0.03037 (D_X/D_{X_0})^{1/2} \text{ cm}]$.

Fig. 2(a) shows the time evolution of activator concentration for the FitzHugh–Nagumo model (FH-N). The concentrations at the node i_1 (curve 1), at the node i_2 (curves 2–3) and at the node i_3 , far behind the barrier (curve 4), as functions of time are presented. Three lower curves show the evolution for the

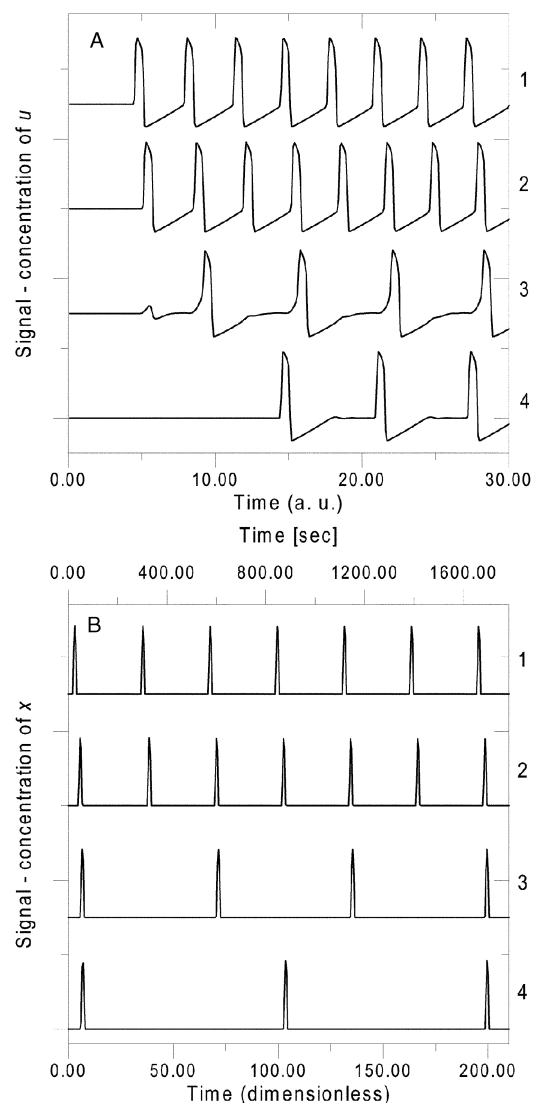


Fig. 2 The time evolution of activator concentration at the node i_1 (curve 1), at the node i_2 (curves 2 and 3) and at the node i_3 (curve 4). The evolutions at i_2 correspond to a narrow, fully transparent barrier (curve 2) and to a barrier for which frequency transformation occurs (curve 3). In the last case the evolution at i_3 for the FH-N model is also shown [curve 4 in part (a)]. In part (b) curve 4 presents the signal observed at i_2 for another width of the passive barrier and illustrates another mode of frequency transforming. (a) The FitzHugh–Nagumo model [eqns. (1)–(4)], $t_p = 3.10$ ($f_1 = 0.323$), $d = 0.063$ (curve 2), $d = 0.169$ (curves 3 and 4). (b) The Rovinsky–Zhabotinsky model [eqns. (5)–(8)], $\tau_p = 32$ ($f_1 = 0.0313$), $d = 2.40 [0.0221(D_X/D_{X_0})^{1/2} \text{ cm}]$ (curve 2), $d = 3.18 [0.0293(D_X/D_{X_0})^{1/2} \text{ cm}]$ (curve 3), $d = 3.24 [0.0299(D_X/D_{X_0})^{1/2} \text{ cm}]$ (curve 4). $\tau_p = 32$ corresponds to 272 s.

following cases: (2) a narrow passive barrier, which is fully transparent; (3) a strip of a width for which the frequency of the outgoing signal is different from the incoming one; and (4) presented to ensure that small maxima of concentration seen on curve 3 do not develop into pulses and that the signal behind the barrier is stable. The evolution at the initial stage of the process is given. The zero of the time scale corresponds to the moment just before the first pulse of the train arrives at the barrier. The results are obtained for $n = 400$, $dl = 0.0211$, $dt = 1 \times 10^{-3}$, $n_1 = 180$, $i_1 = 170$, $i_2 = 190$, $i_3 = 390$ and $f_1 = 0.323$. The value of n_2 is related to the barrier's width. The upper curve (1) corresponds to the incoming signal (input signal at indicator i_1). In the case of $n_2 = 184$ (a narrow, fully transparent passive barrier), all incident pulses observed at indicator i_1 get through the barrier and are also observed at indicator i_2 . Thus, the same signal is observed at indicators

i_1 and i_2 with only a small time shift, which the signal needs to travel over the distance between i_1 and i_2 (curve 2 presents the signal at i_2). However, for a properly chosen width the barrier becomes selective. For $n_2 = 189$ (the barrier's width is then $d = 0.169$) exactly every second one of the incident pulses is transmitted through the barrier and observed at indicator i_2 (curve 3). Therefore, the outgoing signal frequency is half of the original one ($f_2/f_1 = 1/2$). One can see small maxima in the transmitted signal between the big ones on curve 3. However, they do not develop in time into pulses, as the result far from the barrier shows (signal at i_3 —curve 4). We can say that an earlier pulse opens the barrier for the next one and consequently the transformation of frequency occurs for barriers which are wider than the penetration depth.

Results of a similar study for the Rovinsky–Zhabotinsky model [eqns. (5)–(8)] of the Belousov–Zhabotinsky (BZ) system are shown in Fig. 2(b). For this model the first arriving pulse is transmitted, but a number of subsequent ones may be stopped, depending on the barrier's width, so here the earlier pulse passes through and “closes” the barrier. Therefore, the transformation of chemical signal frequency is observed for barriers narrower than the penetration depth. The results presented in Fig. 2(b) have been obtained for $n = 400$, $dI = 0.06$, $d\tau = 1 \times 10^{-3}$, $n_1 = 200$, $i_1 = 150$, $i_2 = 300$ and dimensionless frequency $f_1 = 0.0313$ ($\tau_p = 32.0$, which corresponds to 272 s). The value of n_2 has been changed to describe barriers of various width. The upper curve (1) corresponds to incident pulses (reference signal at indicator 1). For $n_2 = 241$ (a thin, fully transparent passive barrier—curve 2) all incident pulses observed at indicator 1 get through the barrier and are also observed at indicator 2. Thus, the same signal (shifted in time) is observed at indicator 2. For $n_2 = 254$ every second one of the incident pulses is transmitted through the barrier as it is observed at indicator 2 (curve 3). In this case the width of the passive barrier is $3.18 [0.00293 (D_X/D_{X_0})^{1/2} \text{ cm}]$ and the filtering ratio $f_2/f_1 = 1/2$. Further increment in the barrier's width gives smaller filtering ratio. Curve 4 in Fig. 2(b) presents the signal observed at indicator 2 for $n_2 = 255$, which corresponds to $d = 3.24 [0.00299 (D_X/D_{X_0})^{1/2} \text{ cm}]$. For this width of the passive barrier only every third one of the incident pulses is transmitted. Thus the filtering ratio drops to $f_2/f_1 = 1/3$. It worth while to add that results of calculations within the Oregonator model^{24–26} are in qualitative agreement with those for the R-Z model.

In order to learn more about the transformation of signal frequency on a passive barrier, we have performed calculations for different values of t_p and different values of the barrier width d . We have found regimes for which the ratio f_1/f_2 is a small integer number j , which corresponds to a systematic transmission of every j th pulse from a train. The diagrams in the space of parameters (d, t_p) showing “phases” in which the barrier transforms a chemical signal in a given way are shown in Figs. 3 and 4, which describe results obtained for FH-N and R-Z models respectively. The white regions correspond to a given ratio of frequencies (f_2/f_1) of the outgoing (f_2) and incoming (f_1) signals. In the area labelled as “1” every incident pulse is able to get through the passive barrier (the barrier is transparent to all pulses) and the area labelled as “1/2” corresponds to every second one of the incident pulses being transmitted. The grey regions between the labelled areas in Figs. 3 and 4 correspond to more complex (periodic or non-periodic) transmission patterns. For both FH-N and R-Z models, when d increases we observe that the filtering ratio decreases, which means that the pulses are less and less frequently transmitted. Finally the barrier becomes too wide and no pulse can cross it, which corresponds to the area labelled as “0”.

For barriers of width close to the penetration depth (*i.e.* close to the area labelled as “0” in Figs. 3 and 4 the behavior of the FH-N and R-Z models differs. If the time shift between

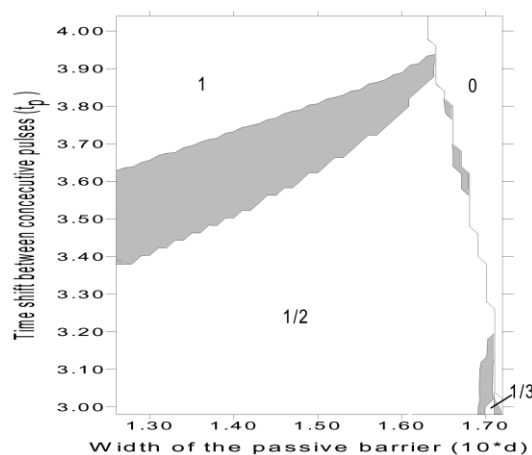


Fig. 3 Filtering ratio (f_2/f_1) for the FitzHugh–Nagumo model as a function of the barrier width (d) and the time shift between consecutive pulses (t_p). The white, labelled areas correspond to the situation when f_2 is the given fraction of f_1 . The grey areas mark more complicated transformations of frequency.

consecutive pulses decreases (the frequency increases) then for the FH-N model the filtering ratio increases, whereas for the R-Z model the filtering ratio decreases. This can be understood from the results shown in Fig. 2. In the case of the FitzHugh–Nagumo model the first incoming pulse makes the barrier more transparent for the subsequent ones. For the Rovinsky–Zhabotinsky model the relaxation of passive area is slower than of the active ones, which makes the strip impenetrable for a later pulse. The results of recent experiments on the BZ reaction show qualitative agreement with the filtering ratio presented in Fig. 4 (*cf.* Fig. 10 in ref. 27).

3 On the response of simple signal processing reactors to regular trains of pulses

Having in mind the results of the previous section one may expect that the properties of signal processing reactors which include a passive barrier should depend on input signal frequency. In this section we discuss the effect of frequency on two such devices.

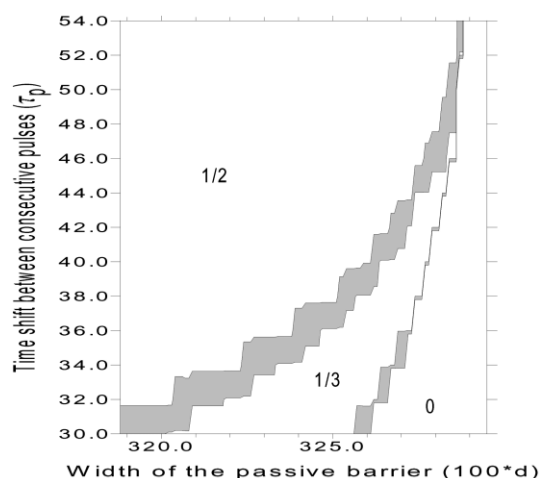


Fig. 4 Filtering ratio (f_2/f_1) for the Rovinsky–Zhabotinsky model as a function of the barrier width (dimensionless d) and the time shift between consecutive pulses (dimensionless τ_p). The white, labelled areas correspond to the situation when f_2 is the given fraction of f_1 . The grey areas stand for more complicated transformations of frequency.

A chemical diode is an asymmetric junction of two active areas, which transmits pulses of excitation coming from one direction and stops those arriving from the other one. The structure of the diode, as proposed by I. N. Motoike and K. Yoshikawa,⁵ is shown schematically in Fig. 5, where the black area stands for the passive medium and the grey areas correspond to the active one. The left edge of the passive region is a straight line, while lines forming a tip of the active region on the right are perpendicular. The shortest distance between the active areas is $d_n > 0$. We assume no flux boundary conditions at all borders of the structure presented in Fig. 5 and free flow between active and passive areas. Plain pulses of excitation may be initiated at the left-hand side border and travel to the right or they can be excited on the right-hand side border and travel to the left. The dashed lines on both sides of the junction, denoted by i_1 and i_2 , mark our new indicators. We study the propagation of pulses through the junction by measuring the mean value of the concentration of the activator (u or x) along these lines. Indicators i_1 and i_2 are located symmetrically with respect to the longitudinal axis of the junction and their length is about half of the width of the whole device. A travelling pulse of excitation may get from one active area to the other one through the passive gap, provided that the gap is not too wide.

Motoike and Yoshikawa⁵ found that the penetration depth strongly depends on the geometry of the boundary between active and passive media. They used the FH-N model [eqns. (1)–(4)] and studied the propagation of pulses in the junction shown in Fig. 5. For the FH-N model, according to the results of Motoike and Yoshikawa,⁵ if the penetration depth for a pulse propagating to the right is denoted by p_d , then the penetration depth for a pulse travelling in the opposite direction is only $0.63p_d$. Results obtained for the passive barrier (d_0 for the FH-N model from Section 2) give $p_d \approx 0.163$. Now building a diode is very easy, because it is sufficient to separate the active areas by a passive field characterized by appropriate d_n , such that $0.63p_d < d_n < p_d$. A similar geometry of the reactor, which works as a signal diode, may be used in the case of the Rovinsky–Zhabotinsky model. For our calculations we have selected $d_n = 3.0$ [$0.02765(D_X/D_{X_0})^{1/2}$ cm], which is slightly smaller than the penetration depth $p_d = 3.295$ [$0.03037(D_X/D_{X_0})^{1/2}$ cm].

The working of a chemical diode is illustrated in Figs. 6(a) and (b) (for the FH-N and R-Z models respectively). In both figures the two upper curves (1 and 2) correspond to a single plain pulse, excited on the left-hand side boundary of the system and travelling to the right. The mean values of activator (u or x) along i_1 (curve 1) and i_2 (curve 2) are plotted as functions of time given along the top axis. The pulse which arrives first at i_1 gets through the passive gap and a moment later it is observed at i_2 (curve 2). The two lower curves (3 and 4) illustrate the propagation of a pulse initiated on the right-hand side boundary and travelling to the left. The mean values of u (or x) along i_2 (curve 3) and i_1 (curve 4) are plotted as functions of

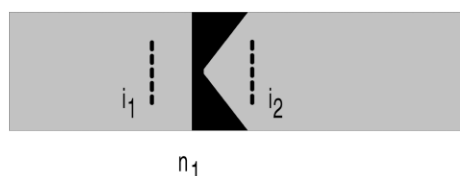


Fig. 5 The scheme of a chemical diode. Lighter areas correspond to active regions, and the black one shows the passive area. The passive gap starts to the right from line n_1 of the grid (excluding n_1). The two dashed lines on both sides of the junction show the position of “indicators”, at which the mean value of u (for the FH-N model) or x (for the R-Z model) as functions of time are recorded. For such a diode geometry a single pulse of excitation may travel through the junction from left to right, but not in the opposite direction.

time shown along the bottom axis. In this case the pulse is first observed at i_2 (curve 3), but then it “dies out” within the passive area (curve 4 is just a straight line). The “chevrons” mark the direction of propagation of the pulses, where the orientation is defined by Fig. 5. In Fig. 6(b) the mean values of x on the indicators are plotted *versus* dimensionless time τ ($\tau = 1$ corresponds to 8.5 s).

The results presented in Figs. 6(a) and (b) have been calculated using the implicit method.²³ For the FH-N model we consider a rectangular area of 4.80×0.9792 covered with a square grid of 251×52 points (including borders, thus $dl = 0.0192$). Indexing the vertical lines of the grid from 0 (left-hand side border) to 250 (right-hand side one) we may specify that indicators are placed along $i_1 = 80$ and $i_2 = 126$. Both of them include 25 nodes. The passive area starts to the right from line $n_1 = 100$ (this line of the grid is still characterized by the active dynamics). The shortest distance between active areas is $d_n = 0.1152$, which is covered by six nodes. We use time integration step $dt = 5 \times 10^{-3}$. For the R-Z model the area of 240×38.25 is covered with a grid of 321×52 points, hence $dl = 0.75$. The other values are respectively: $i_1 = 130$, $i_2 = 175$, $n_1 = 150$ and $d_n = 3.0$ [$0.02765(D_X/D_{X_0})^{1/2}$ cm].

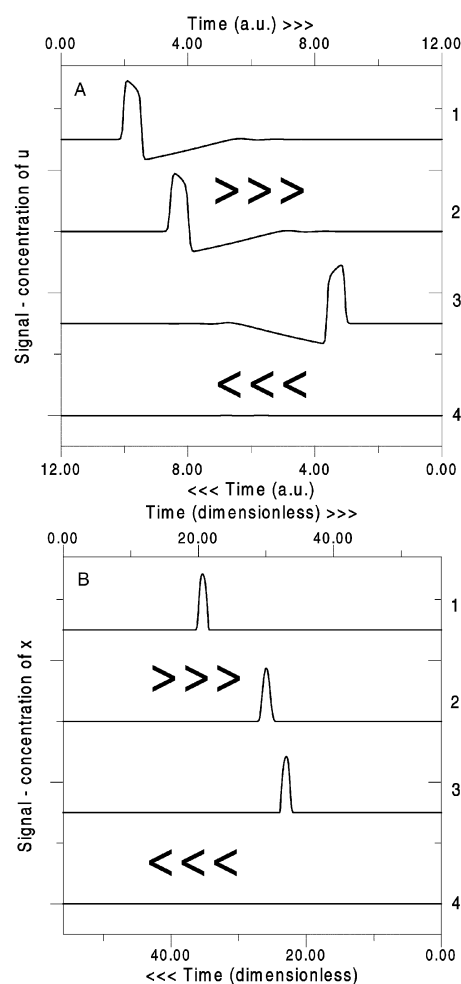


Fig. 6 The time evolution of activator concentration at the indicators i_1 (curves 1 and 4) and i_2 (curves 2 and 3). The two upper curves (1 and 2) correspond to a pulse propagating from left to right (orientation defined by Fig. 5) and the corresponding time scale is along the top axis. In this case the diode transmits the pulse. The two lower curves (3 and 4) correspond to a pulse propagating from right to left (cf. Fig. 5). In this case the pulse is stopped. The “chevrons” mark the direction of propagation. (a) The FitzHugh–Nagumo model, $d_n = 0.1152$. (b) The Rovinsky–Zhabotinsky model, $d_n = 3.0$ [$0.02765(D_X/D_{X_0})^{1/2}$ cm].

$D_{X_0})^{1/2}$ cm—four nodes included]. In this case the time integration step $dt = 1 \times 10^{-3}$.

For the same values of parameters, the calculations for a regular train of pulses arriving at a diode have been performed. The results are presented in Figs. 7(a)–(c), which have exactly the same structure and symbols as Figs. 6(a) and (b).

For the FH-N model we have selected the input signal with frequency $f_1 = 0.278$ (corresponding to the time shift between consecutive pulses $t_p = 3.6$). The time evolutions of concentration at selected nodes are plotted in Fig. 7(a). As expected, the diode is transparent to all the pulses travelling to the right (in the forward direction—curves 1 and 2). However, for the chosen values of parameters we observe that the junction becomes transparent to some of the pulses travelling in the reverse direction (to the left—curves 3 and 4). Therefore, the diode works as a transformer of chemical signal frequency. It is easy to explain this observation. Our barrier ($d_n = 0.1152$) is narrower than the penetration depth in the forward direction ($p_d = 0.163$), and therefore each pulse coming from this direction is transmitted. On the other hand we have selected it as being only slightly wider than the penetration depth in the reverse direction: $0.63p_d = 0.10269$. Consequently, the gap demonstrates the same type of frequency transforming as the passive barrier discussed in the previous section.

For the R-Z model we use the input signal with dimensionless frequency $f_1 = 0.023$ (as the time shift between consecutive pulses is $\tau_p = 44$, i.e. 374 s). The results are plotted in Fig. 7(b). Comparing curves 3 and 4 one can see that in this case the diode stops all the pulses propagating in the reverse direction. As shown in Fig. 6(b) $d_n = 3.0$ is larger than the penetration depth in this direction. The results of Section 2 for the R-Z model (Fig. 4) indicate that such a system becomes less “transparent” at high signal frequency. Therefore it is natural that all pulses propagating in the reverse direction are stopped. However, the diode fails to transmit some pulses propagating in the forward direction (here, the second and fourth ones on curves 1 and 2). Once again the result can be easily explained by what we already know from Section 2. Although $d_n < p_{d,R-Z}$ (as $3.0 < 3.295$), the gap is still in the region for which the frequency transforming in the R-Z model occurs.

When the frequency of the input signal is increased, only the first pulse of the train is able to get through the diode in the forward direction and all subsequent pulses are stopped. This situation is shown in Fig. 7(c), where we use the frequency of the incoming signal $f_1 = 0.05$ ($\tau_p = 20$, corresponding to 170 s).

Fig. 8 presents another structure, being an element of a cross junction,^{8,9} which works as a coincidence detector and as a switch of signal direction. As in Fig. 5, the grey areas correspond to excitable (active) media, while the passive regions have the form of thin strips and are marked with black. Two of these strips are parallel and, together with the excitable medium between them, they form a “channel” inside which excitable pulses propagate. The third strip is set across the channel. We assume free flow between active and passive areas and no flux on the boundaries of the whole structure. If the width of the passive strips is properly chosen, then a pulse travelling along the channel does not “leak out” of it (sideways), but it is able to get through the passive strip perpendicular to the direction of its motion. This characteristic changes when a train of pulses travelling inside a channel is concerned. We have studied the structure shown in Fig. 8 for the FH-N model with the inner width of the channel equal to 1.02 and the width of the passive strips of 0.16 (exactly as in ref. 8), using the implicit method with $d_l = 0.02$ and $dt = 5 \times 10^{-3}$. The pulses are initiated inside the channel, near the left-hand side boundary of the system, and the time shift between consecutive pulses is $t_p = 3.6$. The result is presented in Fig. 9, where lighter shades correspond to higher values of u . It can be seen that the first pulse behaves exactly as expected: it stays within

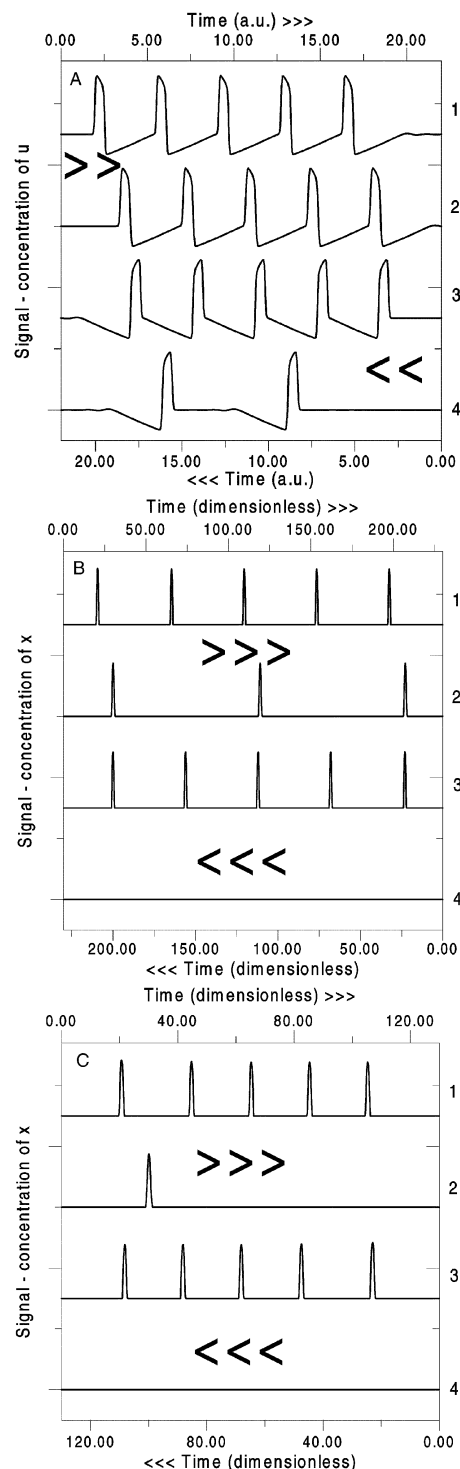


Fig. 7 The time evolution of activator concentration at the indicators i_1 (curves 1 and 4) and i_2 (curves 2 and 3). The two upper curves (1 and 2) correspond to a train of pulses propagating from left to right (orientation defined by Fig. 5) and the corresponding time scale is along the top. The two lower curves (3 and 4) correspond to a train of pulses propagating from right to left (cf. Fig. 5). The “chevrons” mark the direction of propagation. (a) The FitzHugh–Nagumo model, $d_n = 0.1152$, $t_p = 3.60$ ($f_1 = 0.278$). Although the diode still works properly in the forward direction (curves 1 and 2), some pulses may cross it also in the reverse direction (curves 3 and 4). (b) The Rovinsky–Zhabotinsky model, $d_n = 3.0$ [$0.02765(D_X/D_{X_0})^{1/2}$ cm], $\tau_p = 44$ ($f_1 = 0.023$). $\tau_p = 44$ corresponds to 374 s. In this case the diode stops every second pulse travelling in the forward direction (curves 1 and 2), while it works correctly in the reverse direction (curves 3 and 4). (c) The Rovinsky–Zhabotinsky model, $d_n = 3.0$ [$0.02765(D_X/D_{X_0})^{1/2}$ cm], $\tau_p = 20$ ($f_1 = 0.05$). $\tau_p = 20$ corresponds to 170 s. In this case the diode stops all pulses except the first one from a train in the forward direction (curves 1 and 2). It works properly in the reverse direction (curves 3 and 4).

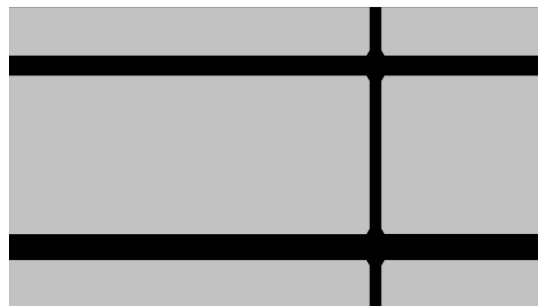


Fig. 8 The scheme of a signal channel. Lighter areas correspond to active regions, and the black areas stand for the passive areas, which have the form of thin strips. Two parallel passive strips together with the excitable medium between them form a channel inside which excitable pulses may propagate.

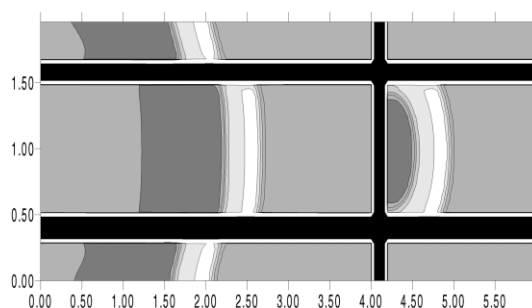


Fig. 9 A snapshot showing the propagation of two consecutive pulses in a signal channel (Fig. 8). Lighter shades correspond to higher concentration of activator (u). This picture is for the FitzHugh–Nagumo model. The width of the passive strips is 0.16, and the width of the active medium inside the channel equals 1.02. The time shift between the pulses is $t_p = 3.60$ ($f_1 = 0.278$). It can be seen that the second pulse “escaped” from the main channel to neighboring areas.

the channel (as the width of the passive strips is just above the penetration depth for a pulse travelling along the strips), but it is able to get through the perpendicular “obstacle” (as the penetration depth in this direction is greater than the width of the passive strips). However, the first pulse “opens” the strips which bound the channel for the following ones. We can see that the subsequent pulse “leaks out” of the channel and excites the neighboring areas (*cf.* the second pulse in Fig. 9). Of course, for the FH–N model all the pulses in a train are able to cross the passive strip perpendicular to the direction of motion.

A similar experiment carried out for the R–Z model with the width of the passive strips of $3.291 [0.030\,34 (D_X/D_{X_0})^{1/2} \text{ cm}]$ and the inner width of the active channel equal to $50.192 [0.4627 (D_X/D_{X_0})^{1/2} \text{ cm}]$ shows that for high frequency signals (*e.g.* for $\tau_p = 20$, corresponding to 170 s) the individual pulses propagate within the signal channel, but some of them may be stopped at the perpendicular passive strip. Thus, the cross junctions described by both FH–N and R–Z types of dynamics are sensitive to the frequency of the input signals.

4 Conclusions

In the paper we discuss the response of simple two dimensional structures composed of active (excitable) and passive areas exposed to regular trains of incoming pulses of excitation. The reactors considered here have been designed for direct processing of information carried by chemical pulses. The chemical diode is an asymmetric junction of excitable fields, in which the propagation of chemical pulses is unidirectional. The cross junction may be used to switch the direction of pro-

pagation of a pulse or as a time coincidence detector. However, it comes out that the operations performed on high frequency trains of pulses may differ from those performed on pulses which are well separated in time. This effect is the result of different evolutions of reagents in passive and active areas, which makes chemical signal processing devices constructed of such areas sensitive to the input signal frequency. We have shown that each passive gap separating excitable areas may act as a transformer of signal frequency.

The mechanism of frequency transforming depends on the system’s dynamics and it is different for the FitzHugh–Nagumo (FH–N) type model and the Rovinsky–Zhabotinsky (R–Z) model of the Belousov–Zhabotinsky (BZ) reaction we have considered in calculations. In the first case the signal transforming properties occur when the first of the incident signals from the train is stopped, but the later ones may go through the barrier, so the frequency transforming is observed for barriers wider than the penetration depth. For the models of the BZ system the first signal is transmitted, but the subsequent ones may be stopped, so the barrier for which frequency transforming occurs should be narrower than the penetration depth. This difference is reflected in qualitatively different responses to a train of pulses given by reactors with the same geometry, but described by FH–N or R–Z models. For example, the chemical diode with dynamics described by the FH–N model becomes transparent to high frequency trains of pulses propagating in the reverse direction. On the other hand, the same diode fails to transmit a high frequency chemical signal in the forward direction when its dynamics is described by the R–Z model of the BZ. Considering the cross junction we observe that for the FH–N model the high frequency chemical signal may escape from the signal channels to the neighboring active areas. Such behavior is not observed for the R–Z model, but in this case the first pulse, which always passes through the junction, may block it for the subsequent pulses coming from the same direction. We also expect that other signal processing devices (logic gates,⁵ memory device⁷) will also exhibit a non-trivial dependence on the input signal frequency.

Acknowledgement

The authors are very grateful to Dr Bartłomiej Legawiec for his advice in the numerical method of solving reaction–diffusion equations used in this study.

References

- (a) A. Hjelmfelt and J. Ross, *Physica D*, 1995, **84**, 180; (b) A. Hjelmfelt and J. Ross, *J. Phys. Chem.*, 1993, **97**, 7988; (c) A. Hjelmfelt, F. W. Schneider and J. Ross, *Science*, 1993, **260**, 335.
- M. Okamoto, Y. Maki, T. Sekiguchi and S. Yoshida, *Physica D*, 1995, **84**, 194.
- O. Steinbock, P. Kettunen and K. Showalter, *J. Phys. Chem.*, 1996, **100**, 18 970.
- A. Toth and K. Showalter, *J. Chem. Phys.*, 1995, **103**, 2058.
- I. N. Motoike and K. Yoshikawa, *Phys. Rev. E*, 1999, **59**, 5354.
- T. Kusumi, T. Yamaguchi, R. R. Aliev, T. Amemiya, T. Ohmori, H. Hashimoto and K. Yoshikawa, *Chem. Phys. Lett.*, 1997, **271**, 355.
- I. N. Motoike, K. Yoshikawa, Y. Iguchi and S. Nakata, *Phys. Rev. E*, 2001, **63**, 036 220.
- J. Siewewiesiuk and J. Górecki, *Acta Phys. Polon. B*, 2001, **32**, 1589.
- J. Siewewiesiuk and J. Górecki, *J. Phys. Chem. A*, 2001, **105**, 8189.
- J. Siewewiesiuk and J. Górecki, *J. Phys. Chem. A*, in the press.
- A. B. Rovinsky, *J. Phys. Chem.*, 1986, **90**, 217.
- A. B. Rovinsky and A. M. Zhabotinsky, *J. Phys. Chem.*, 1984, **88**, 6081.
- R. FitzHugh, *Biophys. J.*, 1961, **1**, 445.
- J. S. Nagumo, S. Arimoto and S. Yoshizawa, *Proc. IRE*, 1962, **50**, 2061.

- 15 R. J. Field, E. Körös and R. M. Noyes, *J. Am. Chem. Soc.*, 1972, **94**, 8649.
- 16 S. K. Scott, *Oscillations, Waves and Chaos in Chemical Kinetics*, Oxford University Press, Oxford, 1994, pp. 27–29.
- 17 A. Lazar, Z. Noszticzius, H.-D. Försterling and Z. Nagy-Ungvarai, *Physica D*, 1995, **84**, 112.
- 18 A. M. Zhabotinsky, F. Buchholtz, A. B. Kiyatkin and I. R. Epstein, *J. Phys. Chem.*, 1993, **97**, 7578.
- 19 L. P. Hammett, *Physical Organic Chemistry. Reaction Rates, Equilibria and Mechanisms*, McGraw-Hill, New York, 1970.
- 20 R. R. Aliev and A. B. Rovinsky, *J. Phys. Chem.*, 1992, **96**, 732.
- 21 M. Frankowicz, A. L. Kawczyński and J. Górecki, *J. Phys. Chem.*, 1991, **95**, 1265.
- 22 K. Miyakawa, F. Sakamoto, R. Yoshida, E. Kokufuta and T. Yamaguchi, *Phys. Rev. E*, 2000, **62**, 793.
- 23 (a) B. Legawiec, private communication; (b) B. Legawiec and D. Ziolkowski, *Inz. Chem. Procesowa*, 1988, **2**, 293 (in Polish).
- 24 J. J. Tyson and P. C. Fife, *J. Chem. Phys.*, 1980, **73**, 2224.
- 25 J. D. Dockery, J. P. Keener and J. J. Tyson, *Physica D*, 1988, **30**, 177.
- 26 R. Toth, A. Papp, V. Gaspar, J. H. Merkin, S. K. Scott and A. F. Taylor, *Phys. Chem. Chem. Phys.*, 2001, **3**, 957.
- 27 K. Suzuki, T. Yoshinobu and H. Iwasaki, *J. Phys. Chem. A*, 2000, **104**, 5154.